Photocurrent Generation in Polymer-Fullerene Bulk Heterojunctions

V. D. Mihailetchi, L. J. A. Koster, J. C. Hummelen, and P. W. M. Blom
Molecular Electronics, Materials Science Centre^{Plus}, University of Groningen, Nijenborgh 4, NL-9747 AG Groningen, The Netherlands
(Received 27 February 2004; published 16 November 2004)

The photocurrent in conjugated polymer-fullerene blends is dominated by the dissociation efficiency of bound electron-hole pairs at the donor-acceptor interface. A model based on Onsager's theory of geminate charge recombination explains the observed field and temperature dependence of the photocurrent in PPV:PCBM blends. At room temperature only 60% of the generated bound electron-hole pairs are dissociated and contribute to the short-circuit current, which is a major loss mechanism in photovoltaic devices based on this material system.

DOI: 10.1103/PhysRevLett.93.216601 PACS numbers: 72.80.Le, 73.61.Ph

Organic photovoltaic devices based on blends of conjugated polymers and fullerene derivatives are considered as promising candidates for photovoltaic applications [1]. The primary process of photocurrent generation is the generation of excitons after absorption of light, either by the donor or by the acceptor. The excitons diffuse in either of the domains towards the polymer-fullerene (donor-acceptor) interface and dissociate via ultrafast electron transfer [2]. After dissociation, a geminate pair of a hole at the donor and an electron at the acceptor is formed. Because of the low dielectric constants ϵ_r of the organic materials (ϵ_r ranges typically from 2 to 4) these electron-hole (*e-h*) or polaron pairs are strongly bound by Coulomb interaction, with binding energies of typically several tenths of an electron volt. In order to generate a photocurrent, the bound *e-h* pairs must dissociate into free charge carriers and subsequently move to the electrodes before recombination processes take place.

In the bulk-heterojunction (BHJ) devices using poly(2-methoxy-5-(3′,7′-dimethyloctyloxy)-*p*-phenylene vinylene) (OC_1C_{10}-PPV) and [6, 6]-phenyl C_{61}-butyric acid methyl ester (PCBM) as donor and acceptor, respectively, an external quantum efficiency of more than 50% and a power conversion efficiency of 2.5% have been reported under simulated solar light [3]. Many fundamental aspects regarding the operation of these devices are presently under strong debate: It has been observed that the photocurrent under short-circuit conditions (J_{SC}) is relatively weakly dependent on temperature [4]. This has been attributed to either the temperature dependence of the charge transport in combination with recombination with shallow traps [5] or space-charge effects [6]. The voltage dependence of the photocurrent in bulk-heterojunction devices has to our knowledge not been addressed; so far only recently a device model for photocurrent in bilayer devices has been developed [7]. Another important issue is the origin of the relatively large external quantum efficiencies in spite of the strong Coulomb binding between the *e-h* pairs in organic materials.

In this Letter a model is presented that consistently explains the voltage and temperature dependence of the photocurrent in PPV:PCBM BHJ devices. It is demonstrated that at voltages V close to the compensation voltage V_0 (V_0-$V < 0.1$ V), implying a small electric field in the device, the photocurrent linearly increases with voltage. For V_0-$V > 0.1$ V the photocurrent enters the saturation regime, as expected for weak recombination. In this regime the photocurrent is governed by the field- and temperature-dependent dissociation of *e-h* pairs according to Onsager's theory of ion pair dissociation [8]. For large (reverse) voltages >10 V the photocurrent becomes field and temperature independent, implying that every generated bound *e-h* pair is dissociated into free carriers by the applied field. The full voltage regime is described by a numerical device model, taking space-charge effects and recombination into account. From the observation of the fully saturated current, we obtain that under short-circuit conditions only 60% of the bound *e-h* pairs in an OC_1C_{10}-PPV:PCBM based photovoltaic device is dissociated.

The measurements were performed on 20:80 weight percentage blends of OC_1C_{10}-PPV:PCBM sandwiched between two electrodes with a different work function to generate an internal electric field, necessary to separate the photogenerated charges. The devices were illuminated by a white light halogen lamp with an intensity of 800 W/m^2, in inert (N_2) atmosphere. A reverse voltage sweep from 1 down to -15 V has been applied and the current density under illumination (J_L) has been recorded for a temperature range of 210–295 K. In order to determine the photocurrent, the current density in the dark (J_D) was also recorded. The experimental photocurrent is given by $J_{ph} = J_L - J_D$. From the resulting J_{ph}-V characteristics the compensation voltage (V_0) at which $J_{ph} = 0$ was determined, as is shown in the inset of Fig. 1. In Fig. 1 J_{ph} at room temperature is plotted on a double logarithmic scale against the effective voltage across the device, given by V_0-V. For a small effective voltage

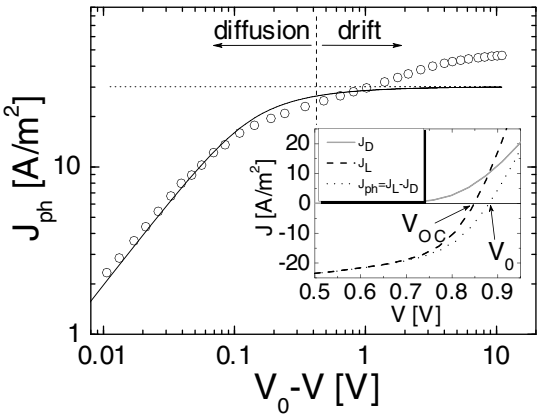

FIG. 1. Room temperature $J_{ph}V$ characteristics of an OC_1C_{10}-PPV:PCBM 20:80 device as a function of effective applied voltage (V_0-V) (open circles), for a device with thickness of 120 nm. The solid line represents the calculated photocurrent from Eq. (1) using $G = 1.56 \times 10^{27}$ m^{-3} s^{-1}, whereas, the dotted line represents the drift current calculated from $J_{ph} = eGL$ using the same G. The inset shows the J_L, J_D, and J_{ph} as a function of bias, whereas the arrows indicate the open-circuit voltage (V_{OC}) and the compensation voltage (V_0), respectively.

(V_0-$V < 0.1$ V) the photocurrent increases linearly with the effective voltage, which has not been noticed before, and then tends to saturate. At higher reverse voltage (V_0-$V > 1$ V) the photocurrent further increases with increasing voltage.

In order to qualitatively understand this behavior, let us first consider the situation in which recombination of free charge carriers as well as space-charge effects can be neglected. In that case, the internal field in the device is given by $E = (V_0 - V)/L$, where V is the applied voltage. Without recombination the photocurrent through the external circuit is $J_{ph} = eGL$ [9], where e is the electric charge, G the generation rate of charge carriers, and L the thickness of the active layer. Thus in case of no recombination and a constant generation rate G of e-h pairs, J_{ph} is independent of V, as shown in Fig. 1 by the dotted line. However, Sokel and Hughes (SH) [10] pointed out that this result is incorrect at low bias voltages because diffusion currents have been neglected. Using the same approximation as above, but including diffusion, SH found an analytical solution for the photocurrent:

$$J_{ph} = eGL\left[\frac{\exp(eV/kT) + 1}{\exp(eV/kT) - 1} - \frac{2kT}{eV}\right], \qquad (1)$$

where eGL is the saturated photocurrent, k is the Boltzmann constant, and T is the temperature. The solutions of $J_{ph} = eGL$ and Eq. (1) are shown schematically in Fig. 1 together with the experimental data. Using a G of 1.56×10^{27} m^{-3} s^{-1}, Eq. (1) fits the experimental data at low effective fields, indicating that diffusion plays an important role in the experimental photocurrent. It should be noted that the photocurrent given by Eq. (1) is independent of the mobility of either electrons or holes, since for none or very weak recombination the carrier lifetime will always exceed the transit time.

It appears from Fig. 1 that for effective voltages exceeding 1 V the experimental photocurrent does not saturate at eGL but gradually increases for larger effective voltages. An important process which has not been taken into account in Eq. (1) is that not all the photogenerated bound e-h pairs (represented by G_{max}) dissociate into free charge carriers. Only a certain fraction of G_{max} is dissociated into free charge carriers, depending on field and temperature, and therefore contributes to the photocurrent (eGL). Consequently, the generation rate G of free charge carriers can be described by

$$G(T, E) = G_{max}P(T, E), \qquad (2)$$

where $P(T, E)$ is the probability for charge separation at the donor-acceptor interface. The photogeneration of free charge carriers in low-mobility materials has first been explained by the geminate recombination theory of Onsager [8]. Onsager calculated the probability that a pair of oppositely charged ions in a weak electrolyte, that undergo a Brownian random walk under the combined influence of their mutual Coulomb attraction and external electric field, would escape recombination. An important addition to the theory has been made by Braun [11], who stressed the importance of the fact that the bound e-h pair (or charge transfer state) has a finite lifetime. The bound e-h pair, formed after the dissociation of an exciton at the donor-acceptor interface, can either decay to the ground state with a rate constant k_F or separates into free carriers with an electric-field-dependent rate constant $k_D(E)$. The decay rate (k_F) is dominated by phonon-assisted nonradiative recombination [12]. Once separated, the charge carriers can again form a bound pair with a rate constant k_R. Consequently, free carriers which are captured into bound pairs may dissociate again during the lifetime of the bound pair. Therefore, long lived charge transfer states act as a precursor for free charge carriers. It has been demonstrated that after generation bound e-h pairs in PPV:PCBM blends can still be detected after microseconds and even milliseconds, depending on temperature [13,14]. Furthermore, Onsager's theory as discussed here was extensively applied in the past to describe photogeneration in pure and sensitized conjugated polymers [15,16]. It should be noted that Onsager's model describes charge dissociation in three dimensions. This is also applicable to bulk-heterojunction cells since the length scale of morphology, typically 2 times the exciton diffusion length (10–15 nm), is in the order of the Onsager radius of 17 nm. In Braun's model the probability that a bound polaron pair dissociates into free charge carries at a given electric field E and temperature T is given by

$$P(T, E) = \frac{k_D(E)}{k_D(E) + k_F}. \quad (3)$$

Based on Onsager's theory for field-dependent dissociation rate constants for weak electrolytes [8], Braun derives $k_D(E)$ for the dissociation of a bound pair to be [11]

$$k_D(E) = k_R \frac{3}{4\pi a^3} e^{-E_B/kT}\left[1 + b + \frac{b^2}{3} + \frac{b^3}{18} + \frac{b^4}{180} + \cdots\right], \quad (4)$$

with a the initial separation of the bound e-h pair at the interface, $b = e^3E/8\pi\epsilon_0\epsilon_r k^2T^2$, and E_B the e-h pair's binding energy. For low-mobility semiconductors electron-hole recombination is given by Langevin: $k_R = e\langle\mu\rangle/\epsilon_0\langle\epsilon_r\rangle$, where $\langle\epsilon_r\rangle$ is spatially averaged dielectric constant and $\langle\mu\rangle$ the spatially averaged sum of electron and hole mobilities. Furthermore, in disorder materials as conjugated polymers and fullerenes it is unlikely that all donor-acceptor separations (a) would be the same [17]. As a consequence, Eq. (3) should be integrated over a distribution of separation distances

$$P(T, E) = N_F \int_0^\infty P(x, T, E)F(x)dx, \quad (5)$$

where $P(x, T, E)$ is the probability that an electron and hole generated at a distance x, temperature T, and field E will escape recombination; $F(x)$ is a distribution function of donor-acceptor separations, and N_F is a normalization factor for the function $F(x)$. The $F(x)$ was assumed to be $F(x) = x^2e^{-x^2/a^2}$, with $N_F = 4/\pi^{1/2}a^3$ [17]. The bulk dielectric constant is $\varepsilon_r = 3.4$ (which was taken as the spatial average dielectric constant of PPV and PCBM). The final parameters required in the model are the mobilities of the charge carriers in the 20:80 blends of OC_1C_{10}-PPV:PCBM, which have recently been determined to be $\mu_e = 2.0 \times 10^{-7}$ m^2/V s [18] and $\mu_h = 1.4 \times 10^{-8}$ m^2/V s [19], at room temperature.

Combining Eqs. (2) and (5), the generation rate of producing free electrons and holes in blends of OC_1C_{10}-PPV:PCBM for any temperature and electric field can be calculated. It should be noted that Eq. (2) involves only two adjustable parameters: the initial separation of e-h pairs a and the ground state recombination rate k_F, since all the other parameters were experimentally determined. Figure 2 shows the calculated photocurrent ($J_{ph} = eGL$, solid lines) as a function of temperature, including the calculated field-dependent generation rate $G(T, E)$. Using $a = 1.3$ nm, and a room temperature recombination lifetime $k_F^{-1} = 1$ μs, the calculations consistently describe the field and temperature dependence of the experimental data in the saturation regime (V_0-$V > 0.3$ V). In the inset of Fig. 2 the spatial distribution $F(x)$ is shown for $a = 1.3$ nm corresponding to a mean e-h separation distance of typically 1.5 nm. In Fig. 3 the (normalized) temperature dependence of the

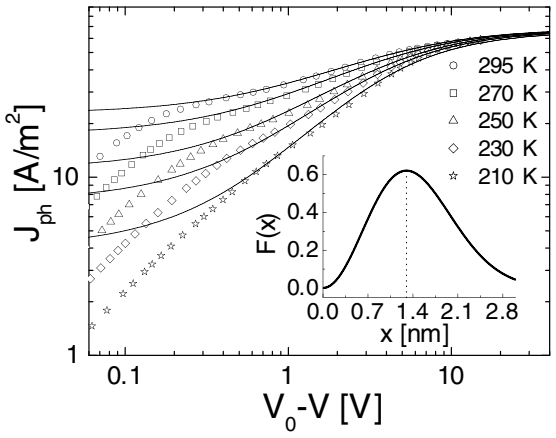

FIG. 2. Temperature dependence of the photocurrent (symbols) versus effective applied voltage (V_0-V) for a device of 100 nm thickness. The solid line represents the calculated photocurrent ($J_{ph} = eGL$) using field-dependent generation rate $G(T, E)$. The inset shows the spatial distribution $F(x)$ for $a = 1.3$ nm.

predicted and experimental photocurrent is plotted, for two different effective voltages of 0.01 V and at short circuit. The excellent agreement at both voltages demonstrates that the activation energy of the photocurrent is completely dominated by the rate of producing free electrons and holes (G) from the internal donor-acceptor interface. It should be noted that the activation energy of G (shown in Fig. 3) arises from the combined effects of the distribution of binding energies, the temperature dependence of both charge carrier mobility and decay rate k_F^{-1}, as well as the effect of applied field, and therefore it does not reflect directly the bound e-h pair activation energy. As shown in Fig. 2, at high effective voltages of typically 10 V, the photocurrent saturates and becomes

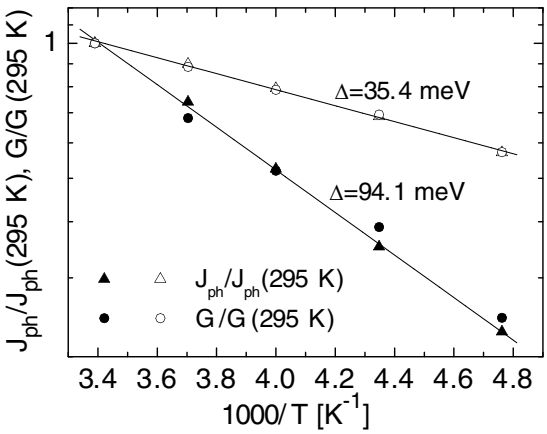

FIG. 3. Normalized experimental photocurrent (J_{ph}) and normalized calculated generation rate [$G(T, E)$] from Fig. 2, as a function of $1/T$, taken in the linear regime at 0.01 V (solid symbols) and at short circuit (open symbols). The activation energies are written on the figure.

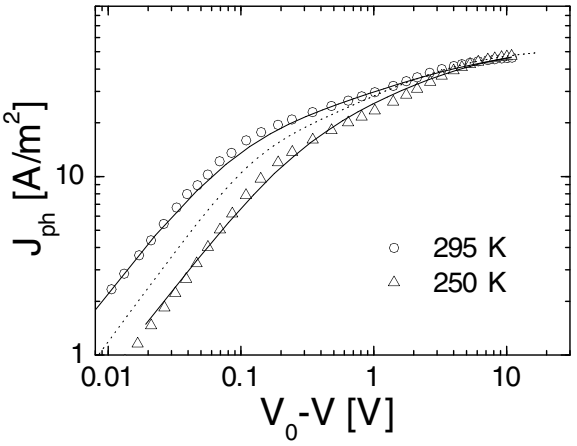

FIG. 4. Experimental photocurrent (J_{ph}) as a function of effective applied voltage (V_0-V) of OC_1C_{10}-PPV:PCBM 20:80 device (symbols), at 295 and 250 K. The solid line represents the numerical calculation including diffusion, field dependent of generation rate $G(T, E)$, and recombination, for a device with a thickness of 120 nm. The dotted line represents calculated J_{ph} from Eq. (1) using $G(T, E)$, at 295 K.

field and temperature independent. At these voltages all bound *e-h* pairs are separated and the maximum photocurrent $J_{sat} = eG_{max}L$ is reached. By comparing the photocurrent with the experimentally observed J_{sat} the dissociation efficiency can be read directly from Fig. 2. Under short-circuit conditions ($V = 0$ V) only 60% of the bound *e-h* pairs dissociate, and at the maximum power point ($V = 0.64$ V) this efficiency even further decreases to 52%. This incomplete dissociation of generated bound *e-h* pairs under operating conditions is therefore a main loss mechanism in solar cells based on PPV:PCBM blends.

As a next step, the generation rate $G(T, E)$ is combined with the Eq. (1), as shown in Fig. 4 by the dotted line, for 295 K. It is observed that this approach underestimates the photocurrent in the low voltage regime. This apparent discrepancy arises from the fact that the analytical model has been deduced for blocking contacts [10]. However, in case of Ohmic contacts (as the devices presented here), the internal electric field in the device is slightly modified due to the band bending created by the accumulation of the charge carries at the interface. This effect is negligible at high reverse bias (in the saturation regime), but it has a significant effect at voltage close to V_0 (in the linear regime). Therefore, the use of Eq. (1) together with $G(T, E)$ will not entirely fit the experimental data of the devices with Ohmic contacts. Furthermore, the analytical model does not include the effects of space-charge and recombination. Therefore, we have developed an exact numerical model that calculates the steady-state charge distributions within the active layer with Ohmic contacts by solving Poisson's equation and the continuity equations, including diffusion and recombination of charge carriers at donor-acceptor interface. This numerical model describes the full current-voltage characteristics in the dark and under illumination, including the field-dependent generation rate $G(T, E)$ [20]. Figure 4 shows the experimental photocurrent (symbols) together with the numerical calculation (solid lines) for two different temperatures. At both temperatures, using the same parameters as presented above, the calculated photocurrent fits the experimental data over the entire voltage range.

In summary, the photocurrent in 20:80 blends of OC_1C_{10}-PPV:PCBM solar cells has been interpreted using a model based on Onsager's theory of geminate charge recombination. The model explains the field and temperature dependence of the photocurrent in a large voltage regime. The long lifetime of 1 μs is a precursor for the high external quantum efficiencies observed in OC_1C_{10}-PPV:PCBM blends. Under short-circuit conditions at room temperature, 60% of the bound *e-h* pairs are separated and contribute to the photocurrent.

The work of L. J. A. Koster forms part of the research program of the Dutch Polymer Institute (#323).

[1] C. J. Brabec *et al.*, Adv. Funct. Mater. **11**, 15 (2001).
[2] C. J. Brabec *et al.*, Chem. Phys. Lett. **340**, 232 (2001).
[3] S. E. Shaheen *et al.*, Appl. Phys. Lett. **78**, 841 (2001).
[4] D. Chirvase *et al.*, J. Appl. Phys. **93**, 3376 (2003).
[5] I. Riedel *et al.*, Adv. Funct. Mater. **14**, 38 (2004).
[6] J. Nelson, Phys. Rev. B **67**, 155209 (2003).
[7] J. A. Barker, C. M. Ramsdale, and N. C. Greenham, Phys. Rev. B **67**, 075205 (2003).
[8] L. Onsager, J. Chem. Phys. **2**, 599 (1934).
[9] A. M. Goodman and A. Rose, J. Appl. Phys. **42**, 2823 (1971).
[10] R. Sokel and R. C. Hughes, J. Appl. Phys. **53**, 7414 (1982).
[11] C. L. Braun, J. Chem. Phys. **80**, 4157 (1984).
[12] N. S. Sariciftci and A. J. Heeger, Int. J. Mod. Phys. B **8**, 237 (1994).
[13] T. Offermans *et al.*, J. Chem. Phys. **119**, 10 924 (2003).
[14] I. Montanari *et al.*, Appl. Phys. Lett. **81**, 3001 (2002).
[15] T. K. Däubler *et al.*, Adv. Mater. **11**, 1274 (1999).
[16] S. Barth and H. Bässler, Phys. Rev. Lett. **79**, 4445 (1997).
[17] T. E. Goliber and J. H. Perlstein, J. Chem. Phys. **80**, 4162 (1984).
[18] V. D. Mihailetchi *et al.*, Adv. Funct. Mater. **13**, 43 (2003).
[19] C. Melzer *et al.*, Adv. Funct. Mater. **14**, 865 (2004).
[20] L. J. A. Koster *et al.* (unpublished).